Breast Cancer (2019) 26:581–593
https://doi.org/10.1007/s12282-019-00957-4

ORIGINAL ARTICLE

Breast cancer cell motility is promoted by 14-3-3γ

Emiko Hiraoka[1] · Takahiro Mimae[1] · Masaoki Ito[1] · Takayuki Kadoya[1] · Yoshihiro Miyata[1] · Akihiko Ito[2] · Morihito Okada[1]

Received: 19 September 2018 / Accepted: 24 February 2019 / Published online: 4 March 2019

Abstract

Purpose Pseudopodia are actin-rich ventral protrusions associated with cell motility and cancer cell invasion. We previously applied our established method of using excimer laser cell etching to isolate pseudopodial proteins from MDA-MB-231 breast cancer cells. We later identified 14-3-3γ as an oncogenic molecule among 46 candidate proteins that are specific to pseudopodia. The present study aimed to determine the function of 14-3-3γ in the motility of breast cancer cells.

Methods MDA-MB-231 cells were cultured on 3-μm porous membranes and double stained to localize 14-3-3γ and phalloidin in pseudopodia using confocal imaging. We assessed pseudopodia numbers and length, as well as migration and wound healing in MDA-MB-231 cells with knockdown and forced expression of 14-3-3γ to determine 14-3-3γ involvement in cell motility. We also immunohistochemically analyzed 14-3-3γ in human breast cancer tissues with high-grade lymphatic invasion.

Results We specifically located 14-3-3γ in pseudopodia of MDA-MB-231 cells. Knockdown and forced expression of 14-3-3γ, respectively, decreased and increased pseudopodial formation and elongation. Migration and wound healing assays also showed that 14-3-3γ knockdown and forced expression, respectively, decreased and increased the number of underside cells and acellular areas in MDA-MB-231 breast cancer cells. More 14-3-3γ was expressed in sites of lymphatic invasion, than in the center and periphery of human breast cancer tissues.

Conclusion The role of 14-3-3γ in breast cancer invasiveness might be to promote cell motility. Inhibition of 14-3-3γ could, therefore, become a novel target of therapy to prevent invasion and metastasis in patients with breast cancers expressing 14-3-3γ.

Keywords Pseudopodia · Metastasis · Triple-negativity · Tumor cell migration · Motility

Introduction

Distant metastasis still interferes with curing breast cancer and other types of carcinoma despite recent therapeutic advances. The initiative metastatic event is to acquire the feature of invasiveness, yet most conventional chemotherapies and molecular target therapies focus on inhibiting cell division and proliferation. To prevent or control invasiveness should offer another way to conquer malignancies; thus, understanding the machinery of cell invasiveness will play a critical role in identifying novel targets of breast cancer therapy.

Pseudopodia are actin-rich protrusions of the plasma membrane that project vertically from a ventral position in cultured cells and play a key role in tumor cell migration and invasion [1–3]. We recently established a means of isolating pseudopodial proteins in which cells are etched using an excimer laser [4, 5]. Two-dimensional difference gel electrophoresis (2D-DIGE) and liquid chromatography coupled with tandem mass spectrometry (LC–MS/MS) analyses of pseudopodial proteins isolated in this manner from MDA-MB-231 human breast cancer cells have identified

Electronic supplementary material The online version of this article (https://doi.org/10.1007/s12282-019-00957-4) contains supplementary material, which is available to authorized users.

✉ Emiko Hiraoka
uenohatunopanda@yahoo.co.jp

[1] Department of Surgical Oncology, Division of Radiation Biology and Medicine, Graduate School of Biomedical and Health Sciences, Hiroshima University, 1-2-3 Kasumi, Minami-ku, Hiroshima City, Hiroshima, Japan

[2] Department of Pathology, Faculty of Medicine, Kinki University, Higashiōsaka, Japan

46 candidate proteins that are specific to pseudopodia [4]. Among them, RAB1A is integrally involved in pseudopodial extension [4, 5]. The expression of RAB1A significantly correlates with tumor size and stage in human lung cancer in vivo [6]. Higher stage, significantly shorter survival, and lymph node and peritoneal metastasis are significantly associated with elevated RAB1A expression in colorectal cancer [7]. In addition, elevated RAB1A expression in gastric cancer is significantly associated with short overall survival [8]. Knockdown of RAB1A inhibits cell migration, cell invasion, and the epithelial–mesenchymal transition (EMT) in triple-negative MDA-MB-231 and BT549 cells in vitro [9]. In addition, α-parvin that also elongates pseudopodia is associated with the lobular carcinoma invasion of lymph nodes in humans [10]. These findings suggest that the proteins identified using our method are promising candidates in terms of associations with invasiveness both in vitro and in vivo.

One of the 46 candidate proteins, 14-3-3γ, belongs to the 14-3-3 family of proteins that is found in all eukaryotic organisms [4]. Seven 14-3-3 isoforms (β, γ, ε, ζ, η, τ and σ) have been identified [11, 12], and they each play key roles in the regulation of various pathways such as cell cycle progression, cell growth, apoptosis, signal transduction and malignant transformation [13–15]. The 14-3-3β, ζ, ε and σ isoforms are involved in cancer progression and migration [16], and 14-3-3β [17, 18] as well as 14-3-3ζ [19] modulate the proliferation and growth of hepatocellular carcinoma (HCC). In addition, 14-3-3ε suppresses E-cadherin [20] and induces focal adhesion kinase expression [21] that induces EMT and HCC migration [20], whereas 14-3-3σ stimulates the expression of heat-shock protein (HSP) 70 that increases HCC cell migration [22]. Also, other 14-3-3 proteins, 14-3-3γ is expressed in HCC [23], lung [24], gastric, colorectal [25] and breast [25, 26] cancers. The expression of 14-3-3γ is involved in the promotion of HCC cell proliferation [27] and its overexpression is associated with extrahepatic metastasis and the overall survival of patients with HCC [28]. The overexpression of 14-3-3γ significantly correlates with lymph node metastasis and distant metastasis of non-small cell lung cancer (NSCLC) [24]. Cell invasion [24] as well as cell proliferation and motility [29] are promoted by 14-3-3γ and its knockdown suppresses EMT [30] in NSCLC cell lines in vitro. These findings indicate that 14-3-3γ also plays a key role in the progression and migration of breast cancer.

Overall survival for patients with breast cancer tumors that express high is worse, compared with low levels of 14-3-3γ [26]. Proximity ligation assays have uncovered significantly more 14-3-3γ/Snail 1 complexes in higher grade, as well as metastatic neck and brain tumors than benign tissues in patients with breast cancer [25]. However, the precise molecular mechanism underlying the involvement of 14-3-3γ in progressive breast cancer, including invasion and metastasis, remains unclear. The present study aimed to determine the role of 14-3-3γ in pseudopodial elongation which is an initiative event in breast cancer cell invasion. Our results implied that 14-3-3γ might serve as a new therapeutic target with which to prevent breast cancer invasion.

Materials and methods

Cell culture conditions and preparation of conditioned medium

MDA-MB-231, MCF7, SKBR3, BT474 human breast cancer cell lines and NIH3T3 fibroblast cells were obtained from the American Type Culture Collection (ATCC, Rockville, MD, USA). We cultured MDA-MB-231 cells in Leibovitz L-15 medium (Life Technologies, Thermo Fisher Scientific, Waltham, MA, USA) supplemented with 10% FBS, 100 units/mL penicillin and 100 µg/mL streptomycin (Invitrogen, Thermo Fisher Scientific), and incubated them at 37 °C in air. We cultured MCF7 cells and BT474 cells in RPMI 1640 medium (Gibco™, Thermo Fisher Scientific) supplemented with 10% FBS, 100 units/mL penicillin and 100 µg/mL streptomycin (Invitrogen), and incubated them at 37 °C in 5% CO_2. SKBR3 and NIH3T3 cells were cultured in Dulbecco's modified Eagle's medium (DMEM) (Nacalai Tesque, Kyoto, Japan) supplemented with 10% FBS, 100 units/mL penicillin and 100 µg/mL streptomycin (Invitrogen), and incubated at 37 °C in 5% CO_2. When NIH3T3 cells reached confluence, the medium was not replaced, and the cells were cultured for another 24 h to prepare conditioned medium, which was passed through 0.45-µm-pore filters and used in the procedures described below [4, 10].

Construction of plasmid vectors expressing 14-3-3γ

Total RNA was extracted from MDA-MB-231 cells using RNeasy Plus Mini Kits (QIAGEN, Hilden, Germany). Full-length cDNA was transcribed from total RNA using Transcriptor First-Strand cDNA Synthesis Kits (Roche Applied Science, Indianapolis, USA) according to the manufacturer's protocol. The cDNA construct for 14-3-3γ inserts was amplified by the polymerase chain reaction (PCR) using KOD FX DNA polymerase (Toyobo, Osaka, Japan) with the following primer set: sense, 5′-CGGGATCCAAGATGGTGG ACCGCGAGCAA-3′ (containing the start codon of 14-3-3γ and a BamHI site) and antisense, 5′-CGGAATTCC AGTTCCCCTGGGGCCTTAAT-3′ (containing an EcoRI enzyme site). The PCR products were resolved by agarose gel electrophoresis and purified using NucleoSpin®Gel and PCR Clean-up (Macherey-Nagel GmbH & Co. KG, Düren, Germany). The cDNA and the pcDNA3.1 (+) vector (Invitrogen) were ligated using Ligation high Ver.2 (Toyobo).

One Shot® TOP10 Chemically Competent *E. coli* (Invitrogen, Thermo Fisher Scientific) was transformed with the plasmid as described by the manufacturer. The plasmid was amplified from cultured *E. coli* using Quantum Prep (Bio-Rad Laboratories, Hercules, CA, USA). The plasmid was extracted, and the accuracy of the constructs was confirmed by sequencing. Plasmids were purified from large-scale *E. coli* cultures using Plasmid Midi Kits (QIAGEN).

Overexpression of 14-3-3γ

MDA-MB-231 cells (4.0×10^5) were seeded in six-well culture dishes and incubated until they reached 50–80% confluence. Thereafter, the cells were transfected for 48 h with plasmid DNA and reagents in Opti-MEM® I Reduced Serum Medium and Lipofectamine® LTX Reagent PLUS™ Reagent (both from Life Technologies) according to the manufacturer's protocol.

Knockdown of 14-3-3γ

MDA-MB-231 cells (3.6×10^5) were seeded in culture dishes and transfected for 48 h with Silencer® Select Validated siRNAs that target 14-3-3γ (s14964, Cat #: 4390824; Ambion, Life Technologies) or control siRNA (In Vivo Negative Control #2 siRNA, Cat #: 4390846; Life Technologies) and Lipofectamine® RNAiMAX Transfection Reagent (Life Technologies) in Opti-MEM® I Reduced Serum Medium (Life Technologies) according to the manufacturer's protocol.

Western blot analysis of 14-3-3γ, RAB1A and the EMT-related protein

Protein lysates of transfected MDA-MB-231, MCF7, SKBR3 and BT474 cells were Western blotted using standard procedures [4] and primary rabbit polyclonal anti-14-3-3γ antibody (C-16:sc-731, Santa Cruz Biotechnology Inc., Dallas, TX., USA), mouse monoclonal anti-RAB1A antibody (G-10:sc-377201, Santa Cruz), mouse monoclonal anti-Fibronectin antibody (EP5:sc-8422, Santa Cruz), mouse monoclonal anti-Vimentin antibody (5G3F10:sc-66002, Santa Cruz), mouse monoclonal anti-E-cadherin antibody (G-10:sc-8426, Santa Cruz), mouse monoclonal anti-β-actin antibody (SLBC3207, Sigma-Aldrich, St. Louis, MO, USA), and secondary rabbit (546, Medical & Biological Laboratories Co., Nagoya, Japan) and mouse (330, Medical & Biological Laboratories Co.) anti-IgG (H + L chain) pAb–HRP antibodies. Proteins on images of Western blots were quantified using Image J software (National Institutes of Health, Bethesda, MD, USA).

Immunostaining and measuring pseudopodial length and density

MDA-MB-231 cells (4.0×10^4) transfected for 48 h were cultured for a further 48 h on 3-μm, porous, polyethylene terephthalate (PET) membranes (353181, BD Diagnostics, Franklin Lakes, NJ, USA) coated with 1 μg/mL of fibronectin (1001859258, Sigma-Aldrich) in 12-well dishes, and pseudopodia were induced to extend into the pores containing NIH3T3-conditioned medium at the bottom. Cells on the membrane were fixed with 4% paraformaldehyde at room temperature for 10 min, washed three times with PBS and incubated in blocking buffer containing 2% BSA in PBS at room temperature for 30 min. The membranes were then immersed in blocking buffer containing 1:50-diluted anti-14-3-3γ antibody (C-16) overnight at 4 °C. After three PBS washes, the cells were incubated with 1:50-diluted Alexa Fluor® 488-conjugated Donkey anti-rabbit IgG antibody (711-545-152, Jackson Immuno Research Laboratories, West Grove, Pennsylvania, USA) in blocking buffer for 2 h at 4 °C. After three PBS washes, the cells were stained with phalloidin (P1951, Sigma-Aldrich) for 30 min at room temperature, washed three times with PBS, mounted on slides and covered with glass coverslips. The cells were assessed by confocal scanning laser microscopy (FV 1000D IX81, Olympus, Tokyo, Japan). Multiple *X*–*Y*-plane images were captured using a 0.3-μm motor step along the *Z*-axis. *Z*-plane views of pseudopodia were reconstructed by stacking *X*–*Y*-plane images. Pseudopodia were counted and their length was measured in cells stained only with phalloidin. The areas of cell types and the lengths of the *Z*-axes of 200 pseudopodia from 30 cells per membrane were measured using Image J software. The density of pseudopodia/mm^2 was determined by dividing the sum of pseudopodia by the sum of the cell area. The mean density and length, and standard error (SE) were calculated from triplicate membranes, and all experiments were repeated three times with comparable results.

Two-chamber transmigration and wound healing assays

Transfected MDA-MB-231 cells (5.0×10^5) were seeded on 8-μm porous PET membranes (353182, Becton-Dickinson, Franklin Lakes, NJ, USA) in 12-well dishes containing NIH3T3-conditioned medium in the bottom of each well for two-chamber transmigration assays. The cells on the membranes were stained with phalloidin for 30 min at 6 and 12 h after seeding. The number of cells on the underside of the

porous membrane was counted per 10 high-power (magnification, 400×) fields using an FV 1000D IX81 confocal scanning laser microscope (Olympus Corporation).

Transfected MDA-MB-231, MCF7, SKBR3 and BT474 cells were cultured in 35-mm μ-dishes with a coverslip-like bottom (Ibidi, Munich, Germany) for wound healing assays. When the cells reached confluence, linear wounds were created by scratching the cell monolayers with the tip of a 200-μL pipet. Images of wounded cells were captured using a microscope equipped with a CCD camera at 0, 6, and 12 h thereafter. Acellular areas were measured using Image J software. The means and SE were calculated from triplicate μ-dishes. Two-chamber transmigration and wound healing assays were repeated three times with comparable results.

Cell proliferation assays

Transfected MDA-MB-231, MCF7, SKBR3 and BT474 cells (1.0×10^5) were seeded in 35-mm μ-dishes with a coverslip-like bottom (Ibidi), then fixed 48 h later with 4% paraformaldehyde at room temperature for 10 min. The cells were washed three times with PBS and incubated in blocking buffer containing 2% BSA in PBS at room temperature for 30 min. The cells were then placed in blocking buffer containing 1:50-diluted mouse monoclonal anti-Ki-67 antibody (MIB-1:sc-101861, Santa Cruz) overnight at 4 °C. After three PBS washes, the cells were incubated with 1:50-diluted Alexa Fluor® 488-conjugated anti-mouse IgG(H + L) and $F(ab')_2$ Fragment antibody (#4408, Cell Signaling Technology, Danvers, USA) in blocking buffer for 2 h at 4 °C. After three PBS washes, the cells were stained with DAPI Fluoromount-G® (Southern Biotech, Birmingham, AL, USA). The cells were counted per 10 high-power (magnification, 800×) fields using an FV 1000D IX81 confocal scanning laser microscope (Olympus). Means and standard errors (SE) were calculated from triplicate μ-dishes. Cell proliferation assays were repeated three times with comparable results.

Patients and tissue specimens

We selected ten patients with high-grade lymphatic invasion (ly3+) diagnosed and treated by surgical resection at Hiroshima University Hospital between September 2016 and March 2018 (Table 1). Tissue specimens were collected from the patients after biopsy or surgery without preoperative chemotherapy. The Institutional Review Board, Ethics Committee for Epidemiology of Hiroshima University approved the protocol (Approval number: 15K19854, hi-160) and waived the requirement for informed consent from the patients.

Immunohistochemistry

Tissue samples were fixed with 10% buffered formalin, embedded in paraffin, and cut into 4-μm sections from selected paraffin blocks. Ten slides were deparaffinized by xylene then rehydrated in ethanol. Antigen was inactivated by autoclaving the slides in 10 nM citrate buffer (pH 6.0) at 104 °C for 40 min. The slides were immersed in 3% hydrogen peroxidase in methanol to block endogenous peroxidase activity for 15 min, followed by 2% BSA in PBS at room temperature for 30 min. The slides were placed in blocking buffer containing 1:20,000-diluted mouse monoclonal anti-14-3-3γ antibody (6A1:sc-69955, Santa Cruz) overnight at 4 °C. After three PBS washes, Dako EnvisionTM + Dual Link System-HRP (Agilent Technologies, Santa Clara, CA, USA) was added, and the slides were incubated at room temperature for 30 min. After three PBS washes, Liquid DAB + Substrate Chromogen System (Agilent Technologies) was applied for 20 s. After three washes with distilled water, the cells were counterstained with Hematoxylin and Eosin Stain Kit (Scy Tek Laboratories Inc., Logan, UT, USA) and observed under light microscopy (ECLIPSE 50i, NIKON, Tokyo, Japan). Staining intensity was visually scored as 0 (negative), 1 (weak), 2 (moderate) and 3 (intense).

Statistical analysis

The density and the length of pseudopodia, as well as the results of two-chamber transmigration assays, cell proliferation assays and Western blots, were analyzed using Welch *t* tests. Wound healing was assessed using Mann–Whitney *U* tests. All data were statistically analyzed using EZR (Saitama Medical Center, Jichi Medical University, Saitama, Japan) [31]. All statistical results were two tailed, and values with $P < 0.05$ were considered significant.

Results

MDA-MB-231 cells contain pseudopodial 14-3-3γ protein

We visualized 14-3-3γ and F-actin in MDA-MB-231 cells by immunofluorescence staining and phalloidin binding, respectively (Fig. 1a–c). MDA-MB-231 cells that had been cultured for 48 h on 3-μm porous membranes were double stained and examined using confocal scanning laser microscopy. Figure 1a–c (upper panel) shows the

Table 1 Clinicopathological characteristics in patients with breast cancer and lymphatic invasion according to location of 14-3-3γ expression

Variable	*n*	14-3-3γ Expression					
		Center		Periphery		Lymphatic invasion	
		Strong	Moderate + weak	Strong	Moderate + weak	Strong	Moderate + weak
Age (years)							
< 50	4	0	4	2	2	2	2
≥ 50	6	0	6	1	5	3	3
Histology							
Solid tubular	1	0	1	0	1	0	1
Scirrhous	9	0	9	3	6	5	4
Clinical stage							
I/II	4	0	4	2	2	2	2
III	6	0	6	1	5	3	3
Pathological tumor size							
≤ 2 cm	3	0	3	1	2	1	2
> 2	6	0	6	2	4	4	2
Unknown	1	0	1	0	1	0	1
Nuclear grade							
1/2	4	0	4	0	4	1	3
3	6	0	6	3	3	4	2
Ki67							
≤ 14%	2	0	2	0	2	1	1
> 14%	8	0	8	3	5	4	4
ER							
(−)	1	0	1	0	1	0	1
(+)	9	0	9	4	5	5	4
PgR							
(−)	1	0	1	0	1	0	1
(+)	9	0	9	4	5	5	4
HER2							
(−)	10	0	10	4	6	5	5
(+)	0	0	0	0	0	0	0
ly							
1+/2+	0	0	0	0	0	0	0
3+	10	0	10	4	6	5	5
v							
(−)	9	0	9	4	5	4	5
1+	1	0	1	0	1	1	0
LN metastasis							
No	2	0	2	1	1	1	1
Yes	8	0	8	2	6	4	4

cytoskeleton and pseudopodia that are rich in F-actin are stained by phalloidin. Pseudopodia appear as dots at the area close to the membrane (Fig. 1b). A *Z*-image shows the projection as pseudopodia by stacking *X*–*Y*-images (Fig. 1c). Phalloidin and 14-3-3γ co-localized on protrusions in the pores. These findings confirmed that 14-3-3γ is specific to pseudopodia.

Numbers and length of pseudopodia are increased by 14-3-3γ

We confirmed 14-3-3γ overexpression and knockdown in MDA-MB-231 cells by immunoblotting (Fig. 2a, b). MDA-MB-231 cells on 3-μm porous membranes were transfected for 48 h, stained with phalloidin and visualized by confocal scanning laser microscopy (Figs. 2c, e, 3a, c). The mean density of pseudopodia per mm^2 was significantly higher in transcribed, than in control cells (14-3-3γ vs. vector: 8506.5 ± 1225.7 vs. 4594.5 ± 222.2, $P = 0.0279$; Fig. 2d) and significantly lower in cells with 14-3-3γ knockdown (si-14-3-3γ vs. si-Control: 2995.6 ± 168.6 vs. 4357.8 ± 526.5, $P = 0.013$; Fig. 2f). Pseudopodia in MDA-MB-231 cells with forced 14-3-3γ expression were obviously longer than those of control cells (mean length; 14-3-3γ vs. vector: 4.48 ± 2.03 vs. 2.96 ± 1.42 μm, $P < 0.01$; Fig. 3b), but significantly shorter in 14-3-3γ knockdown cells (1.90 ± 0.96 vs. 2.68 ± 1.38, $P < 0.01$; Fig. 3d). The results indicated that 14-3-3γ promotes the production and elongation of pseudopodia in MDA-MB-231 cells.

Fig. 2 Immunoblots of 14-3-3γ and β-actin expression show pseudopodial production promoted by 14-3-3γ. Immunoblot targeting (**a**). Bar graphs show mean (with standard error) of 14-3-3γ protein normalized by β-actin (**b**). $^{*}P < 0.05$ and $^{\dagger}P < 0.01$ by Welch *t* tests vs. control (Vector or si-Control) cells. MDA-MB-231 cells were transfected with empty vector (Vector), 14-3-3γ (14-3-3γ), siRNA negative control (si-Control) and siRNA targeting 14-3-3γ (si-14-3-3γ) (**c, e**). Bar graphs of pseudopodial numbers are shown as summed areas of 30 cells (dots/mm^2) Mean density is plotted with bars indicating standard error (**d, f**). $^{*}P < 0.05$ by Welch *t* tests vs. (Vector or si-Control) cells. Bars (**c, e**) 10 μm

MDA-MB-231 cell motility is promoted by14-3-3γ

We assessed whether 14-3-3γ promotes the migration of MDA-MB-231 cells using migration and wound healing

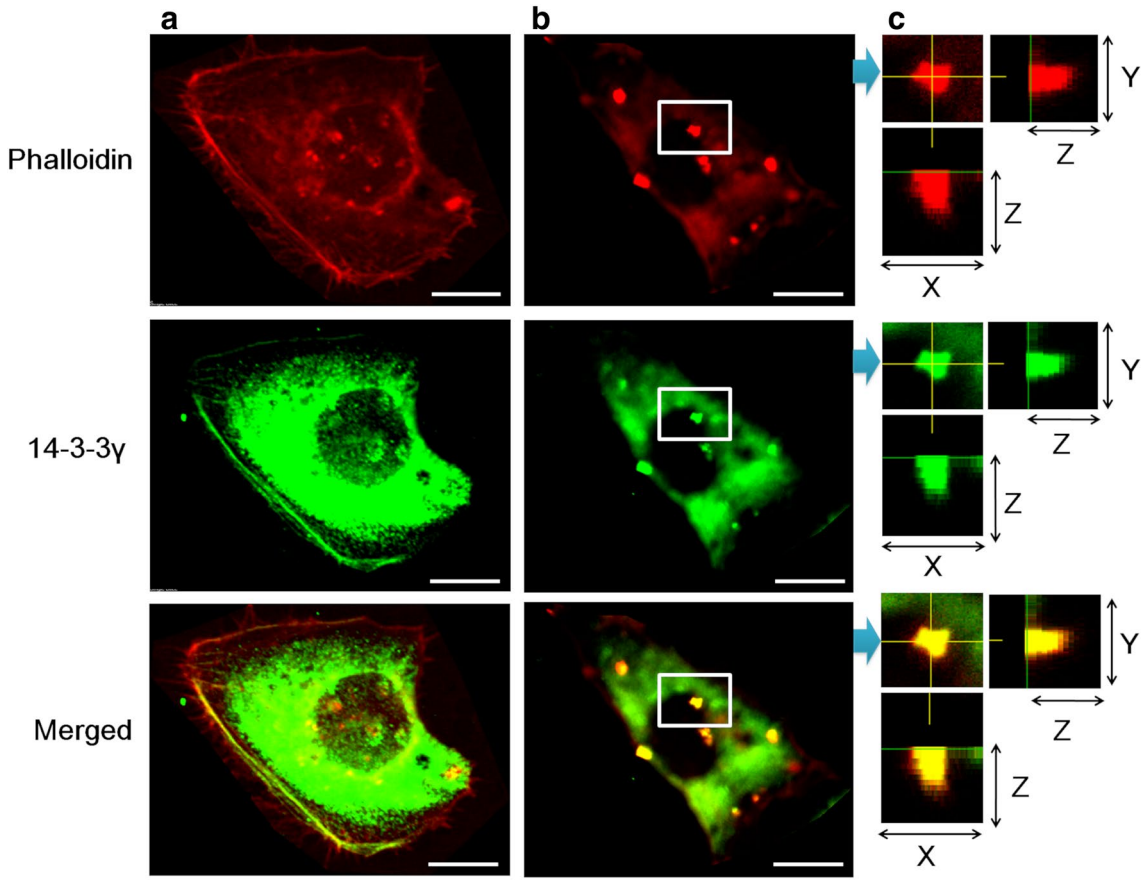

Fig. 1 Subcellular 14-3-3γ localized in MDA-MB-231 cells using confocal scanning laser microscopy. Left row **a**: horizontal cut image at level of visible cytoplasm and nucleus. Middle row **b**: horizontal cut image at level where pseudopodia are evident as dots. Right row **c**: enlargement of image in **b**. Pseudopodia reconstructed in 3D in *XZ*- and *YZ*-directions. Upper columns **a, b**, actin filaments stained with phalloidin. Middle column, 14-3-3γ staining. Lower column, merged upper and middle images. Bars in **a** and **b**, 10 μm

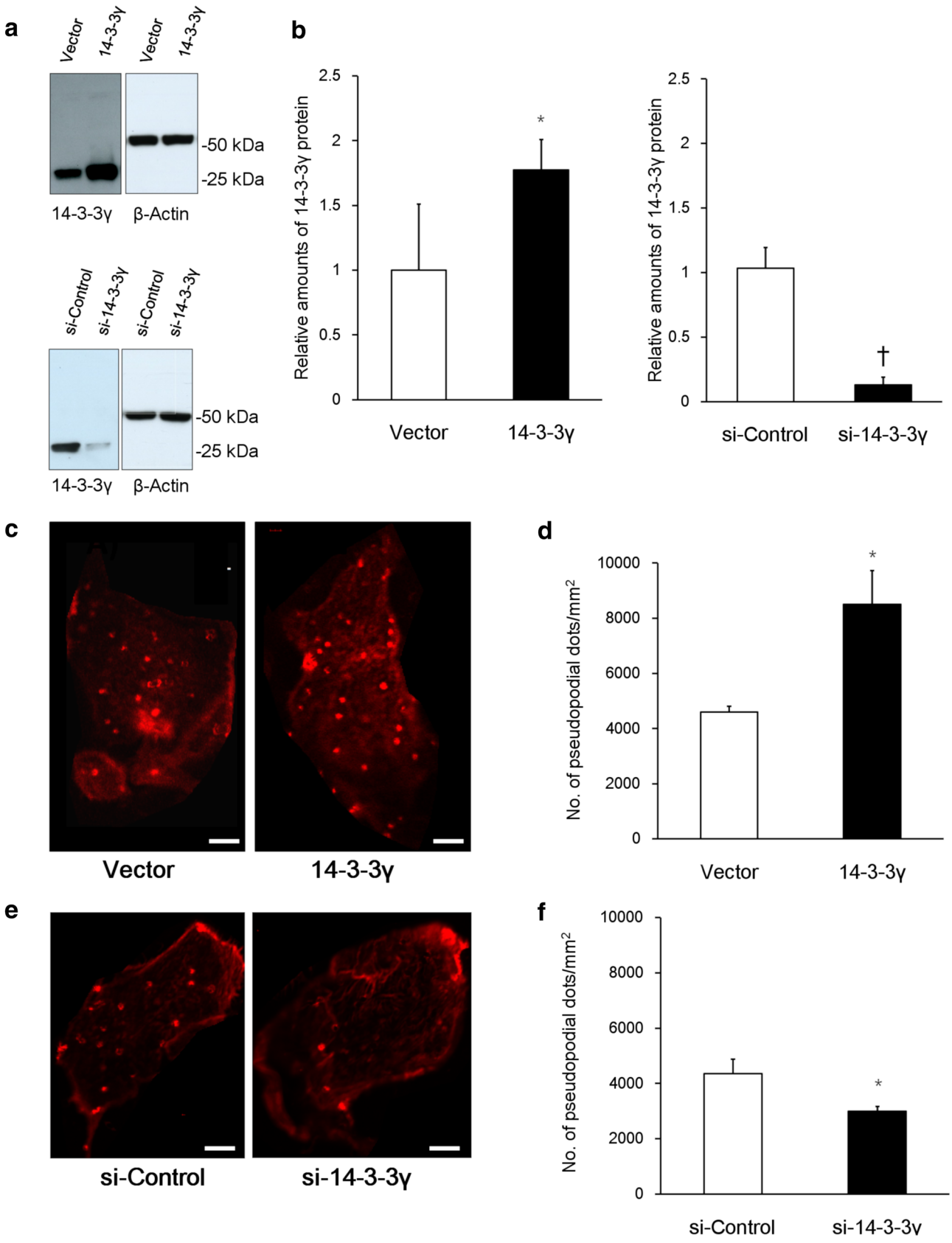
a
Vector
14-3-3γ
Vector
14-3-3γ
-50 kDa
-25 kDa
14-3-3γ
β-Actin
si-Control
si-14-3-3γ
si-Control
si-14-3-3γ
-50 kDa
-25 kDa
14-3-3γ
β-Actin
b
Relative amounts of 14-3-3γ protein
2.5
2
1.5
1
0.5
0
*
Vector
14-3-3γ
Relative amounts of 14-3-3γ protein
2.5
2
1.5
1
0.5
0
†
si-Control
si-14-3-3γ
c
Vector
14-3-3γ
d
No. of pseudopodial dots/mm2
10000
8000
6000
4000
2000
0
*
Vector
14-3-3γ
e
si-Control
si-14-3-3γ
f
No. of pseudopodial dots/mm2
10000
8000
6000
4000
2000
0
*
si-Control
si-14-3-3γ

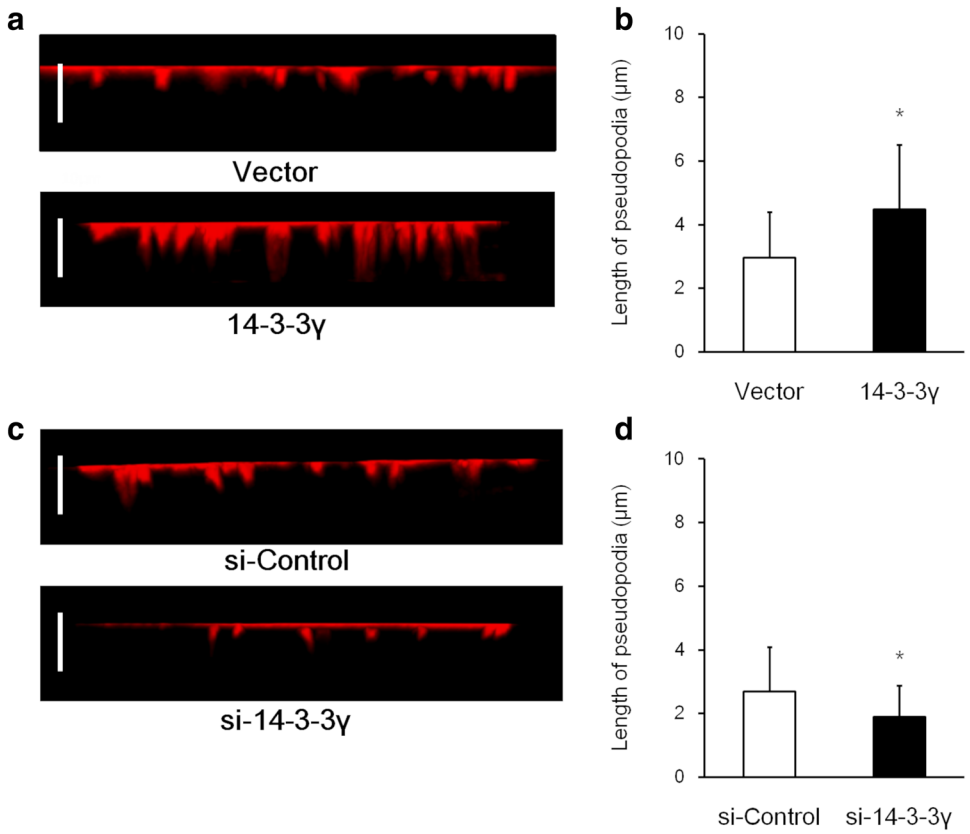

Fig. 3 Pseudopodial elongation is promoted by 14-3-3γ. *Z*-sectional views show pseudopodia in MDA-MB-231 cells with control vector, forced expression and knockdown of 14-3-3γ (**a, c**). Mean lengths plotted with bars indicating standard error (**b, d**). *$P < 0.01$; vs. control cells (Vector or si-Control); Welch t tests. Bars (**a, c**), 10 μm

assays. MDA-MB-231 cells under the membrane that had passed through 8-μm pores by 6 and 12 h were stained with phalloidin and captured by confocal scanning laser microscopy (Fig. 4a, c). More MDA-MB-231 cells/HPF with forced 14-3-3γ expression transmigrated than control cells after 6 and 12 h (mean 14-3-3γ vs. vector at 12 h: 66.9 ± 18.6 vs. 44.1 ± 11.7, $P < 0.01$; Fig. 4b). Conversely, significantly fewer cells with 14-3-3γ knockdown transmigrated than control cells after 6 and 12 h (mean si-14-3-3γ cells vs. si-Control /HPF at 12 h: 28.6 ± 9.0 vs. 51.1 ± 15.1; $P < 0.01$; Fig. 4d).

Acellular areas at 6 and 12 h after scratching were investigated (Fig. 5a, c). Acellular areas were obviously smaller in cells with forced 14-3-3γ expression compared with control cells (mean si-14-3-3γ vs. si-Control: 31.1% ± 12.2% vs. 48.1% ± 9.0%, $P = 0.00183$; Fig. 5b). On the other hand, acellular areas were much larger in knockdown, than in control cells (mean si-14-3-3γ vs. si-Control: 67.2% ± 9.4% vs. 37.9% ± 15.1%, $P < 0.01$; Fig. 5d). Wound healing in MCF7, SKBR3 and BT474 breast cancer cell lines was similar to that in MDA-MB-231 cells (Supplemental Fig. 1). Furthermore, proliferation was assayed in MDA-MB-231, MCF7, SKBR3 and BT474 cells with or without 14-3-3γ knockdown, and almost all types of cells were Ki-67-positive regardless of 14-3-3γ-knockdown (Supplemental Fig. 2). These results suggested that 14-3-3γ promotes breast cancer cell motility, but not proliferation. Western blotting of MDA-MB-231, MCF7, SKBR3 and BT474 cells with or without 14-3-3γ knockdown showed that 14-3-3γ knockdown did not influence the expression of the EMT-related proteins fibronectin, vimentin and E-cadherin (Supplemental Fig. 3). These data indicated that 14-3-3γ is involved in cell motility via other mechanisms.

Elevated levels of 14-3-3γ expressed in lymphatic invasion sites of human breast cancer tissues

Immunohistochemical assessment showed that the amount of 14-3-3γ expressed in sites of lymphatic invasion was equal to or more than that expressed in the center or periphery of tissues derived from 10 human breast cancers with ly3 + lymphatic invasion (Fig. 6a, b). These findings suggested that 14-3-3γ promotes breast cancer cell invasion.

Discussion

This study was based on the identification of a target protein among 46 candidate pseudopodium-specific proteins [4] that were tested to determine whether they are expressed in pseudopodia of MDA-MB-231 breast cancer cells. Confocal

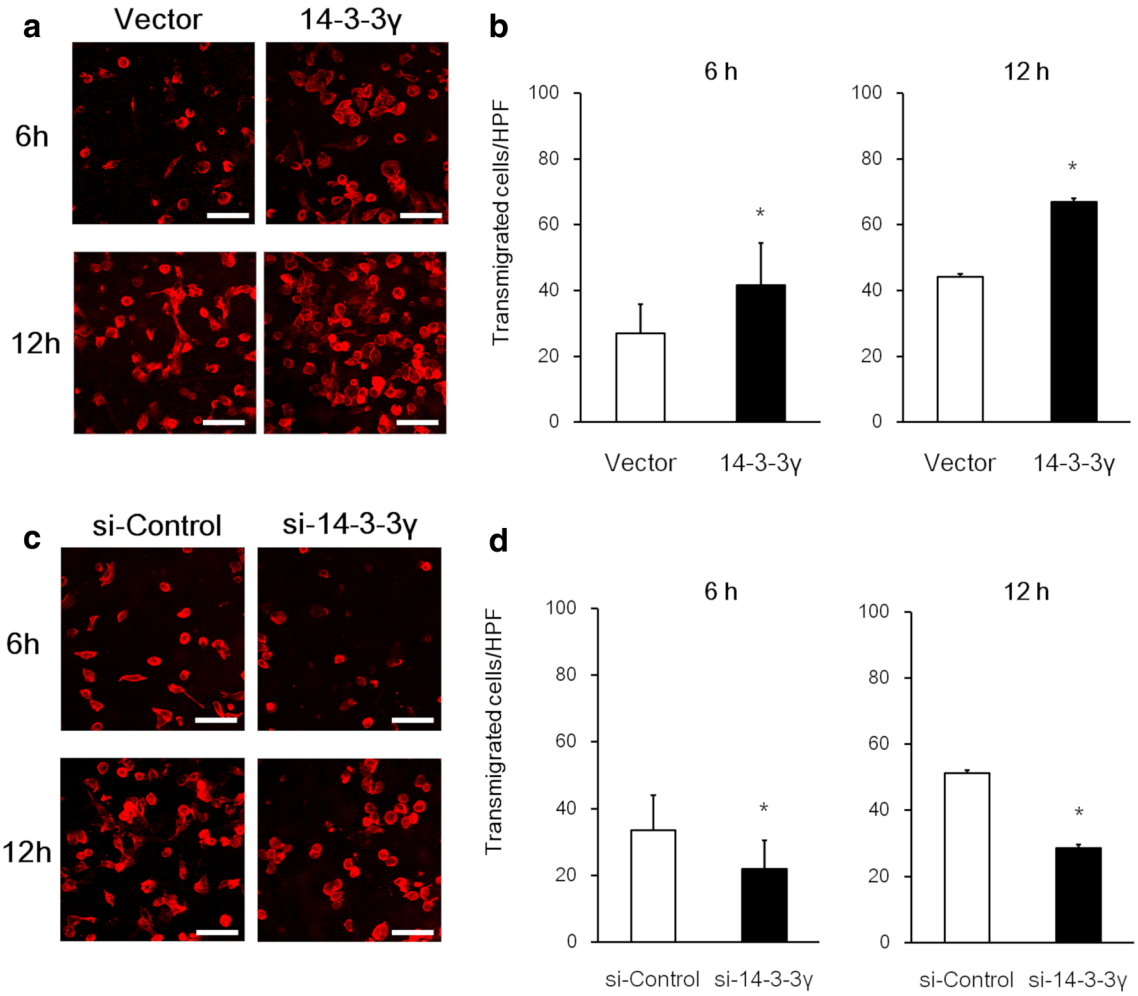

Fig. 4 MDA-MB-231 cell transmigration is promoted by 14-3-3γ. Phalloidin F-actin staining of cells with forced expression and knockdown of 14-3-3γ on 8-μm porous membranes in two-chamber assays at 6 and 12 h after seeding (**a, c**). Bar graphs (**b, d**) show mean number (with standard error) of cells on undersides of membranes. *$P < 0.01$ by Welch t tests vs. Vector or si-Control cells. Bars (**a, c**), 50 μm

imaging showed that pseudopodia were double stained with 14-3-3γ and F-actin 14-3-3γ, indicating that 14-3-3γ is involved in breast cancer cell migration and invasion.

A previous study has shown worse overall survival rates among patients with HCC, NSCLC and breast cancers that express high, rather than low levels of 14-3-3γ [23, 24, 26]. Our results provided one explanation for these findings based on molecular mechanics. Moreover, adenylate energy increased by angiopoietin-like 4 protein enhances EMT by inducing 14-3-3γ expression [25], and Ywhag/14-3-3γ suppresses epithelial gene transcription by forming complexes with Snail 1 in a mouse breast cancer cell line [32]. Knockdown of miR-200c targeting Ywhag/14-3-3γ fundamentally suppresses cell invasion [32]. These previous reports add credence to our results because EMT promotes cancer cell migration and invasion. The present study is the first to show that 14-3-3γ functions in human breast cancer cell migration by elongating and increasing the numbers of pseudopodia as far as we can ascertain. Furthermore, the expression of α-parvin, a candidate pseudopodial protein, correlates with the production of pseudopodia and their ability to migrate [10] and is significantly associated with lymph node metastasis [10]. All patients in the present study had lymphatic invasion of breast cancer and expressed 14-3-3γ in tumors. The intensity of 14-3-3γ was higher at sites of lymphatic invasion than in the center and periphery of tumors. These results together with our findings that pseudopodial numbers and length were quite similar between α-parvin and 14-3-3 γ

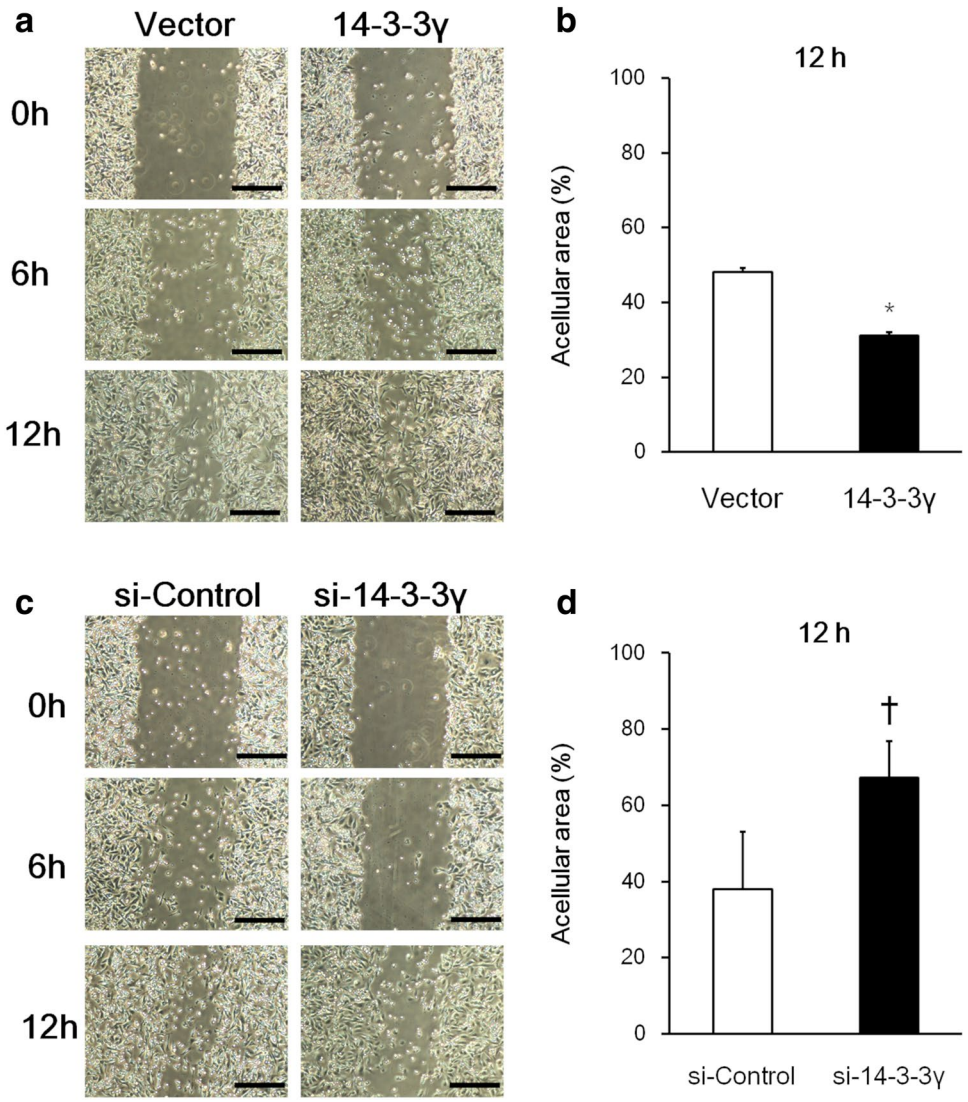

Fig. 5 MDA-MB-231 cell motility is promoted by 14-3-3γ in wound healing assays. Cultured cells with wounds (**a, c**) were harvested at 0, 6, and 12 h after scratching. Bar graphs (**b, d**) represent acellular areas at 12 h divided by areas at 0 h as relative ratios (%) with standard error. $^{*}P < 0.05$ and $^{\dagger}P < 0.01$ by Mann–Whitney *U* test vs. control (Vector or si-Control) cells. Bars (**a, b**), 200 µm

indicate that 14-3-3γ also plays a key role in cancer invasiveness by promoting cell motility.

Although how 14-3-3 γ is associated with other proteins remains unknown, the 46 proteins that are specific to pseudopodia might provide a framework for the initiation of migratory signal transduction based on the results of RAB1A [4, 5], α-parvin [10] and 14-3-3γ. Investigating the relationships between 14-3-3γ and each of the other 45 candidate pseudopodial proteins might reveal a molecular mechanism of cancer cell invasion and migration through inducing motility.

Various strategies have been established to treat breast cancer, but metastatic and recurrent breast cancers remain difficult to cure. The initial event of metastasis is invasion; thus, 14-3-3 γ inhibition might be a new therapeutic target for treating metastatic and recurrent breast cancer. If targeted 14-3-3γ therapy could prevent metastasis and recurrence, invasive breast cancers might be controllable by local surgery and radiation. Recurrent hormone receptor-positive and HER2-positive breast cancers can be prevented by adjuvant therapy. However, an effective systemic therapy has not yet been developed for triple-negative breast cancer (TNBC), which is an aggressive, metastatic malignant subtype of breast cancer with invasive ability. MDA-MB-231 is a TNBC cell line. Thus, inhibitors targeting 14-3-3 γ might pave the way towards novel

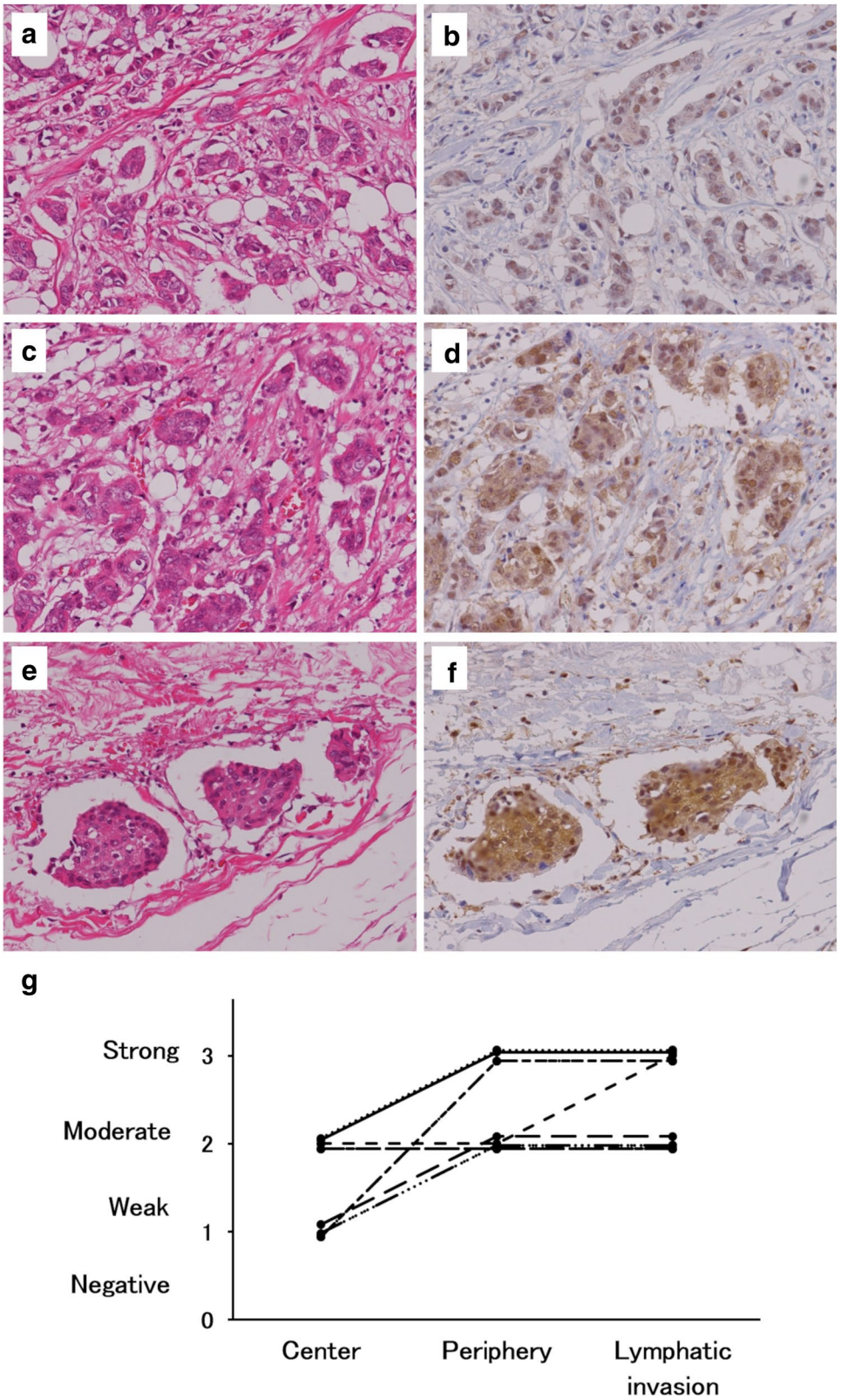

Fig. 6 Immunohistochemistry of 14-3-3γ in human breast cancer. Left row, hematoxylin and eosin stain (**a, c** and **e**, ×200). Right row, immunohistochemical staining for 14-3-3γ (**b, d** and **f**, ×200). Tumor center (**b**) and periphery (**d**) are weakly and moderately stained, respectively, and site of lymphatic invasion (**f**) is intensely stained. Central and peripheral areas of tumor, and site of lymphatic invasion classified according to 14-3-3γ staining intensity (**g**)

treatments for TNBC and highly invasive breast cancers that express elevated levels of 14-3-3 γ.

Acknowledgements The authors thank Yusuke Motoi (Hiroshima University) for technical assistance. Part of this study was supported by the Analysis Center of Life Science, Natural Science Center for Basic Research and Development, Hiroshima University.

Compliance with ethical standards

Conflict of interest The authors have no conflicts of interest to declare.

Ethical approval The Institutional Review Board, Ethics Committee for Epidemiology at Hiroshima University approved this study.

References

1. Guirguis R, Margulies I, Taraboletti G, Schiffmann E, Liotta L. Cytokine-induced pseudopodial protrusion is coupled to tumour cell migration. Nature. 1987;329:261–3.
2. Lauffenburger DA, Horwitz AF. Cell migration: a physically integrated molecular process. Cell. 1996;84(3):359–69.
3. Bravo-Cordero JJ, Hodgson L, Condeelis J. Directed cell invasion and migration during metastasis. Curr Opin Cell Biol. 2012;24(2):277–83.
4. Ito A, Mimae T, Yamamoto YS, Hagiyama M, Nakanishi J, Ito M, Hosokawa Y, Okada M, Murakami Y, Kondo T. Novel application for pseudopodia proteomics using excimer laser ablation and two-dimensional difference gel electrophoresis. Lab Investig. 2012;92(9):1374–85.
5. Mimae T, Ito A. New challenges in pseudopodial proteomics by a laser-assisted cell etching technique. Biochim Biophys Acta. 2015;1854(6):538–46.
6. Wang X, Liu F, Qin X, Huang T, Huang B, Zhang Y, Jiang B. Expression of Rab1A is upregulate in human lung cancer and associated with tumor size and T stage. Aging. 2016;8(11):2790–8.
7. Wang ZK, Cheng ZW, Chen SJ, Zhu XG, Gu YP, Yang XD, Sun L, Liu WT, Zhang YJ, Yuan JF, Tian KJ, Yao YZ, He SB. Aberrant expression of Rab1A and its prognostic significance in human colorectal cancer. Eur Rev Med Pharmacol Sci. 2018;22(14):4509–17.
8. Xu B, Huang C, Yang X, Li X, Li L, Ding Y. Significance and prognostic role of human epidermal growth factor receptor 2 and RAB1A expression in gastric cancer. Oncol Lett. 2018;15(4):5185–92.
9. Xu H, Qian M, Zhao B, Wu C, Maskey N, Song H, Li D, Song J, Hua K, Fang L. Inhibition of RAB1A suppresses epithelial-mesenchymal transition and proliferation of triple-negative breast cancer cells. Oncol Rep. 2017;37(3):1619–26.
10. Ito M, Hagiyama M, Mimae T, Inoue T, Kato T, Yoneshige A, Nakanishi J, Kondo T, Okada M, Ito A. α-Parvin, a pseudopodial constituent, promotes cell motility and is associated with lymph node metastasis of lobular breast carcinoma. Breast Cancer Res Treat. 2014;144(1):59–69.
11. Muslin AJ, Tanner JW, Allen PM, Shaw AS. Interaction of 14-3-3 with signaling proteins is mediated by the recognition of phosphoserine. Cell. 1996;84(6):889–97.
12. Fu H, Subramanian RR, Masters SC. 14-3-3 proteins: structure, function, and regulation. Annu Rev Pharmacol Toxicol. 2000;40:617–47.
13. Dougherty MK, Morrison DK. Unlocking the code of 14-3-3. J Cell Sci. 2004;117(Pt 10):1875–84.
14. Aitken A, Collinge DB, van Heusden BP, Isobe T, Roseboom PH, Rosenfeld G, Soll J. 14-3-3 proteins: a highly conserved, widespread family of eukaryotic proteins. Trends Biochem Sci. 1992;17(12):498–501.
15. Mackintosh C. Dynamic interactions between 14-3-3 proteins and phosphoproteins regulated diverse cellular processes. Biochem J. 2004;381(Pt 2):329–42.
16. Wu YJ, Jan YJ, Ko BS, Liang SM, Liou JY. Involvement of 14-3-3 proteins in regulating tumor progression of hepatocellular carcinoma. Cancers (Basal). 2015;7:1022–36.
17. Liu TA, Jan YJ, Ko BS, Chen SC, Liang SM, Hung YL, Hsu C, Shen TL, Lee YM, Chen PF, Wang J, Shyue SK, Liou JY. Increased expression of 14-3-3β promotes tumor progression and predicts extrahepatic metastasis and worse survival in hepatocellular carcinoma. Am J Pathol. 2011;179(6):2698–708.
18. Sugiyama A, Miyagi Y, Komiya Y, Kurabe N, Kitanaka C, Kato N, Nagashima Y, Kuchino Y, Tashiro F. Forced expression of antisense 14-3-3β RNA suppresses tumor cell growth *in vitro* and *in vivo*. Carcinogenesis. 2003;24:1549–59.
19. Choi JE, Hur W, Jung CK, Piao LS, Lyoo K, Hong SW, Kim SW, Yoon HY, Yoon SK. Silencing of 14-3-3ζ over-expression in hepatocellular carcinoma inhibits tumor growth and enhances chemosensitivity to *cis*-diamminedichloroplatinum. Cancer Lett. 2011;303(2):99–107.
20. Liu TA, Jan YJ, Ko BS, Liang SM, Chen SC, Wang J, Hsu C, Wu YM, Lion JY. 14-3-3ε overexpression contributes to epithelial-mesenchymal transition of hepatocellular carcinoma. PLoS ONE. 2013;8(3):e57968.
21. Ko BS, Jan YJ, Chang TC, Liang SM, Chen SC, Liu TA, Wu YM, Wang J, Liou JY. Upregulation of focal adhesion kinase by 14-3-3ε via NFκB activation in hepatocellular carcinoma. Anticancer Agents Med Chem. 2013;13:555–62.
22. Liu CC, Jan YJ, Ko BS, Liang SM, Chen SC, Lee YM, Liu TA, Chang TC, Wang J, Shyue SK, Sung LY, Liou JY. 14-3-3σ induces heat shock protein 70 expression in hepatocellular carcinoma. BMC Cancer. 2014;14:425. https://doi.org/10.1186/1471-2407-14-425.
23. Lee IN, Chen CH, Sheu JC, Lee HS, Huang GT, Yu CY, Lu FJ, Chow LP. Identification of human hepatocellular carcinoma-related biomarkers by two-dimensional difference gel electrophoresis and mass spectrometry. J Proteome Res. 2005;4:2062–9.
24. Raungrut P, Wongkotsila A, Lirdprapamomgkol K, Svasti J, Geater SL, Phukaoloun M, Suwiwat S, Thonqsuksai P. Prognostic significance of 14-3-3γ overexpression in advanced non-small cell lung cancer. Asian Pac J Cancer Prev. 2014;15(8):3513–8.
25. Teo Z, Sng MK, Lim MMK, Li Y, Li L, Phua T, Lee JYH, Tan ZW, Zhu P, Tan NS. Elevation of adenylate energy charge by angiopoietin-like 4 enhances epithelial-mesenchymal transition by inducing 14-3-3γ expression. Oncogene. 2017;36(46):6408–19.
26. Song Y, Yang Z, Ke Z, Yao Y, Hu X, Sun Y, Li H, Yin J, Zeng C. Expression of 14-3-3γ in patients with breast cancer: correlation with clinicopathological features and prognosis. Cancer Epidemiol. 2012;36(6):533–6.
27. Ajjappala BS, Kim YS, Kim MS, Lee KY, Ki HY, Cha DH, Baek KH. 14-3-3γ is stimulated by il-3 and promotes cell proliferation. J Immunol. 2009;182(2):1050–60.
28. Ko BS, Lai IR, Chang TC, Liu TA, Chen SC, Wang J, Liou JY. Involvement of 14-3-3γ overexpression in extrahepatic metastasis of hepatocellular carcinoma. Hum Pathol. 2011;42(1):129–35.
29. Wang P, Deng Y, Fu X. MiR-509-5p suppresses the proliferation, migration, and invasion of non-small cell lung cancer by targeting YWHAG. Biochem Biophys Res Commun. 2017;482(4):935–41.
30. Raungrut P, Wongkotsila A, Champoochana N, Lirdprapamomgkol K, Svasti J, Svasti J, Thonqsuksai P. Knockdown of 14-3-3γ

suppresses epithelial-mesenchymal transition and reduces metastatic potential of human non-small cell lung cancer cells. Anticancer Res. 2018;38(6):3507–14.
31. Kanda Y. Investigation of the freely-available easy-to-use software "EZR" (Easy R) for medical statistics. Bone Marrow Transpl. 2013;48(3):452–8.
32. Perdigão-Henriques R, Petrocca F, Altschuler G, Thomas MP, Le MT, Tan SM, Hide W, Lieberman J. miR-200 promotes the mesenchymal to epithelial transition by suppressing multiple members of the Zeb2 and Snail1 transcriptional repressor complexes. Oncogene. 2016;35(2):158–72.